

Photochemistry of large ring 2-phenylcycloalkanone in the presence of molecular oxygen

著者	Takahashi Kazuya, Watanabe Takeyuki, Kohtani Shigeru, Nakagaki Ryoichi
journal or publication title	Journal of Photochemistry and Photobiology A: Chemistry
volume	186
number	2-3
page range	290-297
year	2007-02-01
URL	http://hdl.handle.net/2297/3632

doi: <https://doi.org/10.1016/j.jphotochem.2006.08.021>

Photochemistry of Large Ring 2-Phenylcycloalkanone in the Presence of Molecular Oxygen

Kazuya Takahashi, Takeyuki Watanabe, Shigeru Kohtani, and Ryoichi Nakagaki*

Graduate School of Natural Science and Technology, Kanazawa University, Kakuma-machi, Kanazawa 920-1192, Japan

Abstract

Photolysis of 2-phenylcyclododecanone (2PCDD, ring size: C₁₂) has been investigated in an air-saturated solution. The α -photocleavage of 2PCDD (Norrish type I) has led to the formation of triplet acyl-benzyl biradical (³BR) which reacts with O₂ to produce a peroxyester intermediate. A major photoproduct of 2-phenyl-1-oxacyclododecane is formed by a stepwise decarboxylation from the peroxyester intermediate. The peroxyester is also a common intermediate for minor products of benzaldehyde, cyclodecane, and acetophenone. 1-Phenylcycloundecane is produced from decarbonylation of ³BR. On the other hand, ³BR undergoes intersystem crossing to the singlet biradical which in turn recombines to form the parent 2PCDD or to afford a cage product of cyclophane. The recombination yield to the starting species is estimated to be 0.5 by measuring a time evolution of enantiomer concentration of 2PCDD starting from one optically pure enantiomer. Photolysis mechanism of 2PCDD in the presence of molecular oxygen has been proposed and discussed.

Keywords: Cyclic ketone, Norrish type I photolysis, Biradical, Photooxidation, Molecular oxygen

Corresponding author Tel./Fax: +81 76 234 4425

E-mail address: nakagaki@p.kanazawa-u.ac.jp (R. Nakagaki)

1. Introduction

Norrish type I (photochemical α -cleavage) reactions of cyclic ketones have been extensively studied in photochemistry and spin chemistry associated with magnetic field and magnetic isotope effects on chemical reactions as well as chemically induced dynamic nuclear and electron spin polarization (CIDNP and CIDEP) [1 – 12]. The photochemical reactions mainly lead to the formation of triplet biradicals from triplet excited state of cyclic ketones, which results in the formation of singlet biradicals through spin conversion processes such as intersystem crossing (ISC). Cage products are formed from the intramolecular (unimolecular) reaction of singlet biradical, while escape ones can be produced in an intermolecular (bimolecular) reaction of triplet biradical with a parent molecule in the ground state or other radical scavengers (e.g. O₂). The competition between the intra- and intermolecular photoreactions may depend on the applied field strength, because the ISC rate can be sensitive to the magnetic field [12 – 16].

In 1972, the photolysis of 2-phenylcyclopentanone (C₅) and 2-phenylcyclohexanone (C₆) have been reported by Baum, in which alkenals were obtained in high yields (>80%) [17]. Several years later, Doubleday has found that magnetic fields affect the CIDNP signals of ¹³C carbonyl carbons of 2-phenylcycloalkanones (2PCAs) (C₆-C₈) as well as photoproducts of alkenals and ketenes [3]. This result suggests that the ISC of acyl-benzyl biradicals is influenced by external magnetic fields. In succession, Turro, Doubleday and co-workers have vigorously studied magnetic field and chain length effects on the lifetime of acyl-benzyl biradicals [4 – 7]. They have also found the formation of cyclophanes in the photolysis of large ring 2PCAs (C₁₀-C₁₆) [5 – 7]. The product yield of cyclophanes depends on the ring size of 2PCAs. Scheme 1 shows the photochemical pathway of 2PCAs in degassed solutions.

In the presence of molecular oxygen, 2PCAs afford several products through different processes. We have recently reported that the triplet acyl-benzyl biradicals (C₆-C₈) react with molecular oxygen to produce benzoylalkanoic acids, which can be further excited by the UV light, and then subsequent intramolecular hydrogen abstraction (Norrish Type II) occurs to produce acetophenone and the corresponding alkenoic acids [18]. Turro et al. have observed enhanced ¹³C CIDNP signals at carbonyl carbon on the products in

the photolysis of 2-phenylcyclododecanone (2PCDD) in aerated solution, in which the presence of an oxidized peroxyester or peracid species has been suggested [6]. Interestingly, the ^{13}C CIDNP signal from carbon dioxide has been observed, which may be evolved by the decarboxylation on the peroxyester or peracid species in the 2PCDD photolysis.

This paper is concerned with the Norrish Type I photolysis of 2-phenylcyclododecanone (2PCDD), especially, focused on the escape process of the triplet acyl-benzyl biradical (^3BR) with molecular oxygen. Time profiles of the product formation have been examined on the basis of product identification and quantification on gas chromatography/mass spectrometry (GC/MS). Yield of recombination from the singlet acyl-benzyl biradical (^1BR) to the parent 2PCDD has also been determined by measuring time evolution of enantiomer concentration of 2PCDD starting from one optically pure 2PCDD enantiomer [18]. From these results, we will discuss the photolysis mechanism of 2PCDD in the presence of molecular oxygen. In addition, this paper deals with magnetic field effects (MFE) on the end product yields in the photolysis of 2PCDD. It is interesting to examine the possibility because the ISC rate from ^3BR to ^1BR have been changed in the applied magnetic field [4,5].

2. Results

2.1. Optical and chiroptical properties

The absorption and CD spectra of 2PCDD are shown in Figure 1. The absorption spectrum mainly consists of a broad $n\pi^*$ band of carbonyl group in 280-330nm region and a vibronic $\pi\pi^*$ band of phenyl group ($^1A_{1g} \rightarrow ^1B_{2u}$) around 260nm. The primarily forbidden $n\pi^*$ band of the carbonyl group is slightly more intense than that of $\pi\pi^*$ transition of phenyl group. This is explained by an enhanced $n\pi^*$ transition probability due to an interaction of the $\pi\pi^*$ and $n\pi^*$ transitions dependent on relative location of the carbonyl bond with respect to the aromatic ring [19]. The $n\pi^*$ band of the carbonyl group mainly contributes to the CD spectra of 2PCDD. Although 2PCDD was completely resolved using our chiral HPLC method, the sign of the CD spectra has not yet been correlated with the absolute stereochemical

configuration of 2PCDD.

2.2. Biradical lifetime

Transient absorption signals of the benzyl radical moiety (320nm) on ^3BR were measured by means of the laser flash photolysis upon the 308nm excitation. The obtained transient signals of decay component of ^3BR were well fitted with $\text{Abs}(t) = A + B \exp(-t/\tau)$, where $\text{Abs}(t)$ is the transient absorption intensity, A and B are time-independence constants, and τ is the lifetime of ^3BR . If the rates of recombination and/or cage reactions from ^1BR is much faster than that of the reverse ISC, the rate constant of ISC (k_{ISC}) corresponds to reciprocal of τ in degassed sample. Figure 2 shows MFE dependence on the relative value of ISC rate constants ($k_{\text{MF}}/k_{0\text{T}}$), where $k_{0\text{T}}$ is the ISC rate constant at 0 mT ($1.3 \times 10^7 \text{ s}^{-1}$) and k_{MF} is the rate constant in a magnetic field. The MEF dependence curves show a maximum (1.15) at 5 mT followed by a decrease to an asymptotic value (ca. 0.7) in high field region ($> 100 \text{ mT}$). This result is in accord with that reported by Turro and coworkers [4,5]. The observed MFE are explained in terms of the hyperfine coupling (HFC) interaction and S-T. level crossing mechanism [4,5,12,16]. The peak at 5 mT on the ISC rate arises from the T₋-S degeneracy due to the Zeeman splitting of the triplet sublevels since the singlet level lies slightly below the triplet ones in the acyl-benzyl biradical from 2PCDD. In the high field region ($> 100 \text{ mT}$), the Zeeman splitting for T₊ and T₋ becomes sufficiently large not to interact with the singlet state.

In order to confirm the reaction between ^3BR and O₂, the transient absorption measurement was carried out in air-saturated solutions. The value of τ in the aerated sample solution (τ_{air}) for 2PCDD has been determined to be 37 ns. In this condition, the reciprocal of τ_{air} is expressed as $1/\tau_{\text{air}} = k_{\text{ISC}} + k_{\text{ESC}}[\text{O}_2]$, where k_{ESC} is a bimolecular rate constant and $[\text{O}_2]$ is the O₂ concentration in solution. Since $[\text{O}_2]$ is 3.1 mM in hexane at 20 - 25°C [20], k_{ESC} is evaluated to be $4.5 \times 10^9 \text{ M}^{-1}\text{s}^{-1}$, indicating that ^3BR undergoes a diffusion-controlled reaction with O₂.

2.3. Photoproducts in the presence of molecular oxygen

Figure 3 indicates GC/MS total ion chromatogram of the air-saturated sample after 10 min irradiation with

high pressure Hg lamp (> 290 nm), where the extent of 2PCDD decomposition was 93 %. Minor peaks with short retention times of 7.8, 10.9, and 12.9 min are assigned to benzaldehyde, acetophenone, and cyclodecane, respectively. Peaks **1** and **2** are attributed to the product of 2-phenyl-1-oxacyclododecane **1** and phenylcycloundecane **2** by a comparison with the synthesized authentic samples. Peak **3** is identified as cyclophane **3**. The product **1** as well as the minor products of benzaldehyde, acetophenone, and cyclodecane have been observed in the aerated solution, whereas they are never produced in degassed samples. On the contrary, the peak intensities of the product **2** and **3** are increased for degassed samples, while these are drastically diminished in an O_2 saturated solution. Other peaks are still unidentified at present.

Time profiles of decomposition of 2PCDD and formation of **1** in the air-saturated solution are depicted in Figure 4 (a). While 2PCDD is completely decomposed within 40 min irradiation, concentration of **1** is increased and becomes 0.56 mM at 40 min. This result indicates that **1** is the main product in the photolysis of 2PCDD in the presence of O_2 . Figure 4 (b) illustrates evolutions of **2**, benzaldehyde, cyclodecane, and acetophenone with the irradiation time. Yields of these products are about one order of magnitude smaller than that of **1**. It should be noted that the time profiles of the product **2**, benzaldehyde and cyclodecane are very similar to that of **1**. On the other hand, the evolution of acetophenone is quite different to those of the other products; there is an induction period (ca. 5 min) in acetophenone formation. The concentration of acetophenone increases more slowly than those of other products, and may further increase after 40 min. Figure 4 (c) indicates the time profile of cyclophane formation, in which the vertical axis shows relative peak intensities on the GC/MS measurement. The peak intensity of cyclophane rapidly grows up, and then gradually decreases. This suggests that the cyclophane slowly undergoes decomposition under the irradiation condition.

Magnetic field effects on the end product yields have also been examined in the air-saturated samples after 5 min irradiation. Here, the extent of 2PCDD decomposition is ca. 80%. Table 1 summarizes concentrations and yields of **1** and **2** as well as the relative peak intensity of **3**. The applied magnetic fields were set at 5, and 600 mT, because k_{MF}/k_{OT} shows the maximum (1.15) and minimum (0.7), respectively.

The values listed in Table 1 coincide within the experimental error, i.e., MFE on the end-product yields have not been observed.

2.4. Time evolution of enantiomer concentration

We estimated the recombination yield of 2PCDD in the same manner as reported in our previous paper [18]. This estimation is based on the measurement of time evolution of 2PCDD enantiomers starting from the one optically pure enantiomer. Since linearly polarized light (LPL) was used in this work, molar extinction coefficients of the two enantiomers are equal. Therefore, the differential equations (7) and (8) described in the reference [18] are rewritten as follows:

$$\frac{d[R]}{dt} = -1000I_0\eta \left\{ 1 - 10^{-\varepsilon([R]+[S])} \right\} \left(\frac{[R]}{[R]+[S]} - \frac{k_{ISC}}{k_{ISC} + k_{ESC}[O_2]} \phi \right)$$

$$\frac{d[S]}{dt} = -1000I_0\eta \left\{ 1 - 10^{-\varepsilon([R]+[S])} \right\} \left(\frac{[S]}{[R]+[S]} - \frac{k_{ISC}}{k_{ISC} + k_{ESC}[O_2]} \phi \right)$$

where $[R]$ and $[S]$ are concentration of the R and S enantiomers, respectively. I_0 is an incident light intensity ($\text{einstein} \cdot \text{s}^{-1} \text{cm}^{-2}$), ε is the molar extinction coefficient of 2PCDD at 308 nm ($\text{M}^{-1} \text{cm}^{-1}$), η is a quantum yield of ^3BR generated from the excited 2PCDD, and ϕ is a recombination yield from ^1BR to each 2PCDD enantiomer. Observed time profiles of the two enantiomers were simulated by integrating the above two differential equations by the Runge-Kutta method. Here, ε , k_{ISC} , and $k_{ESC}[O_2]$ are fixed to the values obtained from our absorption and transient absorption measurements, whereas $I_0\eta$ and ϕ were varied as fitting parameters. Figure 5 shows the time evolution of the enantiomer concentrations of 2PCDD with LPL irradiation. It is obvious that as the one enantiomer concentration decreases, the other enantiomer concentration increases to reach the maximum value, and then decrease. Finally, both enantiomer concentrations coincide asymptotically. This result clearly indicates that the photo-induced racemization of 2PCDD occurs via the recombination of ^1BR . The sum of the recombination yield of ^1BR to each 2PCDD enantiomer (2ϕ) can be estimated to be 0.5 on the basis of simulation.

3. Discussion

Scheme 2 illustrates the photochemistry of 2PCDD in the presence of molecular oxygen. The photoexcited 2PCDD firstly undergo the α -cleavage to give ^3BR . Deactivation processes of ^3BR should be composed of the following three different pathways: (1) the escape process with molecular oxygen to produce **1**, benzaldehyde, cyclodecane, and acetophenone, (2) the thermal decarbonylation to form **2**, and (3) the intersystem crossing to yield ^1BR followed by the production of **3** and the recombination to yield 2PCDD.

In the escape process (1), the benzyl radical moiety on ^3BR would firstly react with O_2 followed by affording the peroxyester intermediate **4** as shown in Scheme 2. The transient absorption measurement indicates that the reaction rate of the benzyl radical moiety with O_2 ($k_{\text{ESC}}[\text{O}_2] = 1.4 \times 10^7 \text{ s}^{-1}$) is almost comparable to that of ISC ($k_{\text{ISC}} = 1.3 \times 10^7 \text{ s}^{-1}$). Therefore, more than a half amount of ^3BR undergoes the oxidative radical reaction with O_2 in the air-saturated condition. After O-O dissociation of the intermediate **4**, decarboxylation from the biradical **5** occurs to give the main product of **1**. Such a stepwise decarboxylation from the peroxyester **4** is favorable for generating primary alkyl radicals as reported by Buback and coworkers [21, 22]. The product yield of **1** shows the considerably high value (0.56) for 40 min irradiation, which may be due to the efficient decarboxylation and recombination to the biradical **6** as well as the effective reproduction of 2PCDD from ^1BR (the recombination yield is 0.5). The biradical **6** can also afford benzaldehyde and cyclodecane, though the yields of these products are quite smaller than that of **1**. The time profiles for formation of **1**, benzaldehyde, and cyclodecane closely resemble each other, suggesting that the rate determining step of these products is at the O-O bond dissociation of the intermediate **4**. Turro et al. have suggested the presence of the intermediate **4** based on the CIDNP measurement of the 2PCDD photolysis in the presence of O_2 [6]. They have observed the production of carbon dioxide derived from the carbonyl carbon attached in 2PCDD molecule. These observed results are well explained by Scheme 2. On the other hand, acetophenone may be produced from **7** as reported in our previous paper [18]. In this case, **7** can be excited by the UV light and then undergoes the subsequent intramolecular hydrogen abstraction (Norrish Type II) to form acetophenone and 9-decenoic acid. The induction period in the

acetophenone formation can be explained by the secondary photoreaction of **7**.

The decarbonylation process (2) from ^3BR is worth while to consider. It has been reported by Miranda et al. [23] that phenylcycloalkanes were produced in the intense laser photolysis of smaller ring 2PCAs ($\text{C}_6\text{-C}_8$). They have claimed that the photochemistry of 2PCAs includes a two-photon process, where the decarbonylation from 2PCAs has occurred upon the two-photon process with an intense pulsed laser. However, we have demonstrated in this study that the decarbonylation of ^3BR can proceed thermally upon the steady state photolysis of 2PCDD. Consequently, the two-photon decarbonylation is not necessarily to produce phenylcycloalkane **2** from 2PCDD. The thermal decarbonylation of acyl radicals has been well studied, which are reviewed by Vollenweider and Paul [24]. The rate constants to form primary alkyl radicals from the corresponding acyl radicals on the thermal decarbonylation are in the range of $10^5 - 10^6 \text{ s}^{-1}$ at 298 K. These values are about one or two order of magnitude smaller than that of the escape reaction with O_2 , which leads the formation of cyclic ether **1**. Therefore, it is quite reasonable to obtain the product yield of **2** (ca. 0.03) about one order of magnitude smaller than that of cyclic ether **1** (0.56) after 40 min irradiation.

The cage recombination yield of ^1BR has not been determined for 2PCDD. The rate constants for recombination of the biradical species ($\text{C}_6\text{-C}_8$) has been estimated theoretically by de Kanter and Kaptein [25] based on Doubleday's CIDNP data [3]. We have also estimated the recombination yields for 2PCAs ($\text{C}_6\text{-C}_8$ and 2PCDD) by the different approach described in a previous paper [18]. The recombination yield (0.5) for 2PCDD obtained in this study is smaller than those (0.8 - 1.0) for smaller ring 2PCAs ($\text{C}_6\text{-C}_8$). This can be explained by the existence of cyclophane formation from ^1BR for 2PCDD. Nevertheless, the cage recombination of ^1BR to reproduce 2PCDD may greatly contribute to the high yield of cyclic ether **1**.

No magnetic field effects on the end product yield were found for 2PCDD by comparing the peak intensities of the products **1**, **2**, and **3** in the GC/MS measurement, though MFE on the ISC rate of acyl-benzyl biradical has been observed [5, 6]. In general, MFE on the end product yield are relatively difficult to observe, because competition between the cage and the escape product formation is necessary [12 - 16]. In this case, this requirement is almost fulfilled, since the escape rate from ^3BR is comparable to that of ISC in air-saturated condition. A possible explanation for the absence of MFE is that the rate determining

step may not be the ISC process of the acyl-benzyl biradical derived from 2PCDD. This can be true for cyclic ether **1**, because the rate determining step is possibly at the O-O bond dissociation of the intermediate **4**. On the other hand, since the rate of cage reaction from ^1BR to cyclophane **3** is sufficiently larger than that of ISC [5], the ISC process should be the rate limiting step for the production of cyclophane **3**. The variation range of $k_{\text{MF}}/k_{\text{OT}}$ (0.7 – 1.15) would be enough to observe MFE on the product yields beyond experimental errors. The absence of MFE for cyclophane **3** might be due to the subsequent secondary photodecomposition of **3** in the continuing irradiation condition. In the case of the product **2**, the thermal decarbonylation of ^3BR leads to the formation of alkyl-benzyl biradical **8** which may exhibit larger MFE on the lifetime of the biradical **8** because of possessing carbon centered radicals on both radical moieties [9, 12, 26]. Therefore, MFE on the product yield of **2** was greatly expected, but this result is contrary to the expectation.

The MFE on the ISC rate of acyl-benzyl biradical has been observed for 2PCDD in this work and in the previous study by Doubleday and Turro [4,5], whereas no MFE has been detected for the small ring 2PCAs ($\text{C}_6\text{-C}_8$) [18]. This can be explained by the predominance of the field-independent spin-orbit coupling (SOC) mechanism over the field dependent HFC one in the ISC process of acyl-benzyl biradicals [4,5]. Doubleday and Turro have claimed that SOC plays a major role in the ISC process because of delocalization of the odd electron on the acyl oxygen. In general, it is recognized that if radical pairs are separated by 1 nm or more, the singlet-triplet energy gap is decreased and the ISC is controlled by HFC [5, 12, 16]. However, SOC interaction will exponentially increase with decreasing radical pair distance so that contribution of magnetic-field-dependent HFC to the ISC becomes much smaller in such a short chain biradical. Consequently, ISC will be completely dominated by SOC in the acyl-benzyl biradicals derived from small rings ($\text{C}_6\text{-C}_8$), thereby diminishing MFE.

4. Experimental

4.1. Materials

Benzaldehyde (Nacalai Tesque, 98%), acetophenone (Katayama Chemical, 98%), and cyclodecane (Tokyo Kasei, 98%) were purchased and used without further purification. Hexane of HPLC grade (Nacalai Tesque) was used as received.

4.1.1. Preparation and optical resolution of 2PCDD

2PCDD was prepared according to the procedure described by Han et al [7], and characterized by ¹H-NMR, MS, UV, and IR spectroscopy. The physical properties are in full agreement with those reported in ref. [7]. Optical resolution of 2PCDD were conducted on a HPLC system (Waters 510 pump, a Yamato BU150A oven and Waters Lambda-Max Model 481 detector) equipped with a normal-phase chiral column (Daicel Chiralcel OJ-H 4.6mm i.d. × 15 cm). A mixture of 2-propanol/hexane (9:1) was used as an eluent at the flow rate of 0.8mL min⁻¹.

4.1.2. Preparation of 2-phenyl-1-oxacyclododecane

2-Phenyl-1-oxacyclododecane **1** was synthesized according to Scheme 3. 10-Undecenal (1.0 g, 5.9 mmol) was treated with 13 mL of 0.94 M (12.2 mmol) solution of phenyllithium in 50 mL of THF at -78°C under Ar, and the purification was carried out by column chromatography (SiO₂, 9% ethyl acetate in hexane) to yield 1.0 g of alkenol **9** (71%). The olefinic alcohol **9** (2.0 g, 8.1 mmol) was treated with 10 mL of 1.15 M solution of borane in THF (which is diluted with 50 mL of THF) in an ice bath for 2 h. The solution was then allowed to warm to room temperature. To this solution was added 2 mL of water, 3 mL of 3 M NaOH, then 1 mL of 30% H₂O₂, and then stirred for 1 h in the 50°C oil bath. The purification was carried out by column chromatography (SiO₂, 33% ethyl acetate in hexane) to yield 1.7 g of diol **10** (78%). A mixture of **10** (1.47 g, 5.6 mmol), zinc chloride (0.77g) and 111 mL of chloroform was refluxed for 2 h, diluted with chloroform, and then washed with water and brine. The organic layer was dried over anhydrous MgSO₄.

The resulting crude **1** was purified by column chromatography (SiO₂, 9% ethyl acetate in hexane) to yield 0.14 g of colorless solid (10% yield); m.p. 33 – 35 °C; UV $\lambda_{\text{max}}/\text{nm}$ (Hexane, ϵ) 252 (380); ¹H-NMR (500MHz, CDCl₃): δ = 7.24(m, 5H), 4.14(dd, J = 8.06 Hz, 2.81 Hz, 1H), 3.62(t, 1H), 3.25(t, 1H) 1.64-1.18(m, 18H); IR(KBr) 2917, 2851, 2359, 2327, 1459, 1065, cm⁻¹; MS: m/z 246(M⁺); Found: C, 82.67; H, 10.92%. Calcd. for C₁₇H₂₆O: C, 82.87; H, 10.64%.

4.1.3. Preparation of 1-phenylcycloundecane

1-Phenylcycloundecane **2** was synthesized by the catalytic hydrogenation of 1-phenylcycloundecene. 1-Phenylcycloundecene (prepared according to the paper by Han et al. [7], 0.8 g, 3.3 mmol) was treated with 24 mg of 10% Pd-C under atmospheric pressure hydrogen in ethyl acetate for 4 h. The solution containing **2** was filtrated, evaporated, and the crude **2** was purified by column chromatography (SiO₂, hexane) to yield 1.0 g of colorless oil (79% yield); m.p. -36 - -33 °C; UV $\lambda_{\text{max}}/\text{nm}$ (Hexane, ϵ) 259 (207); ¹H-NMR (500MHz, CDCl₃): δ = 7.23(5H,m), 2.80(1H, m), 1.83-1.36(20H,m); IR(KBr) 3084, 3061, 3026, 2927, 2862, 1603, 1494 cm⁻¹; MS: m/z 230(M⁺); Found : C, 88.39 ; H,11.57%. Calcd. for C₁₇H₂₆ : C, 88.62; H, 11.38%.

4.2. Spectroscopic measurements

UV absorption spectra were measured on a spectrophotometer (Hitachi U-3210). Circular dichroism (CD) spectra were obtained on a spectropolarimeter (JASCO J-820).

4.3. Transient absorption measurements

Deaerated 1.2 mM hexane solution of 2PCDD were degassed by several freeze-pump-thaw cycles. The experimental apparatus for transient absorption measurements has been reported in our previous papers [18, 26]. All of the measurements were carried out at ambient temperature.

4.4. Steady-state photolysis of 2PCDD with high-pressure mercury lamp

Concentration of air-saturated 2PCDD solution was 1.0 mM in hexane. Degassed or O₂ saturated

solution was prepared by bubbling pure N₂ or O₂ gas for 30 min before irradiation. The sample solution (4.0 mL) in a quartz cell (1.0 × 1.0 × 4.5 cm) was placed between the pole pieces of an electromagnet (Tokin SEE-9G), and irradiated with UV light from a 500W high-pressure mercury lamp (Ushio USH-500D) equipped with a glass filter (Toshiba UV-29) at ambient temperature. The cage product of cyclophane was isolated from the irradiated solution by column chromatography (SiO₂, 2% ethyl acetate in hexane); ¹H-NMR (500 MHz, CDCl₃): δ = 7.73(d, J=8.3Hz, 2H), 7.28(d, J=8.3Hz, 2H), 2.89(t, 2H), 2.69(t, 2H), 1.67(m, 4H), 1.40-0.79(m, 14H); MS: m/z (relative intensity) 90(22), 118(45), 131(100), 146(47), 187(17), 230(M⁺, 33). These data are in good agreement with those reported by Han et al.[7].

Photoproduct analyses were carried out on a GC-MS instrument (Hewlett-Packard 6890/5973) equipped with a capillary column (Agilent HP-5MS, 30 m × 0.25 mm i.d., film thickness 0.25 μm). Helium carrier gas was used with linear velocity of 30 cm s⁻¹. A sample solution (2 μL) with an internal standard of anthracene was injected with a split ratio of 50:1. The injector temperature was 250°C, and the column temperature was kept at 50°C for the first 2 min and then increased at the rate of 5°C min⁻¹ to 250°C. The mass spectrometer was set to scan mass units 40 – 550 for electron impact ionization with a source temperature of 230 °C.

4.5. Pulsed laser photolysis of 2PCDD with linearly polarized light

The XeCl pulsed laser beam (Lambda Physik CompEX 100, at 308 nm, fwhm ca. 14 ns) was converted into linearly polarized light (LPL) by passing through a circular iris (φ = 10 mm) and a polarizer (Sigma Koki, laser prism, 10 × 10 mm, 21 mm thick). The average output of the final polarized light was ca. 0.35 mJ cm⁻²pulse⁻¹. An air-saturated 2PCDD solution in a cylindrical quartz cell (φ 10 mm × 10 mm path length) was placed between the pole pieces of an electromagnet (Tokin SEE-9G). Time evolution of enantiomer concentration of 2PCDD starting from one optically pure enantiomer was determined by using the same chiral HPLC system for the optical resolution of 2PCDD as described in this experimental section.

5. Conclusions

The present study has revealed outline of overall photolysis mechanism of 2PCDD in aerated solutions. In the escape reaction of triplet acyl-benzyl biradical (^3BR) with O_2 , the decomposition of cyclic peroxyester intermediate **4** is suggested. The products of 2-phenyl-1-oxacyclododecane **1**, benzaldehyde, cyclodecane, and acetophenone are probably formed via the intermediate **4**. Among these products, the cyclic ether **1** especially exhibits the high yield (0.56), which may be due to the efficient decarboxylation from the intermediate **4** as well as the reproduction of parent 2PCDD through ISC from ^3BR to the singlet ^1BR followed by the cage recombination. The cage recombination yield of ^1BR has been estimated to be 0.5 by measuring a time evolution of enantiomer concentration of 2PCDD starting from one optically pure enantiomer. The absence of MFE on the end product yields indicates that the photolysis of 2PCDD in the presence of O_2 proceeds in somewhat complicated manner.

Acknowledgment

This work was supported by Grant-in Aids for Scientific Research (No. 15750030 and No. 18550011) from the MEXT of Japan. One of the authors (S. K.) is also grateful to the financial support from the Mitsubishi Chemical Corporation Fund.

References

- [1] N.J. Turro, *Modern Molecular Photochemistry*, Benjamin/Cummings, Menlo Park, 1978, Chap. 8.
- [2] F.J.J. de Kanter, R. Kaptein, and R.A. van Santen, *Chem. Phys. Lett.* 45 (1977) 575-579.
- [3] C. Doubleday Jr., *Chem. Phys. Lett.* 64 (1979) 67-70.
- [4] M.B. Zimmt, C. Doubleday Jr., N.J. Turro, *J. Am. Chem. Soc.* 107 (1985) 6726-6727.
- [5] C. Doubleday, Jr., N.J. Turro, J.F. Wang, *Acc. Chem. Res.* 22 (1989) 199-205, and references cited therein.
- [6] N.J. Turro, K.C. Hwang, V.P. Rao, C. Doubleday Jr., *J. Phys. Chem.* 95 (1991) 1872-1879.
- [7] N. Han, X. Lei, N.J. Turro, *J. Org. Chem.* 56 (1991) 2927-2930.
- [8] O.B. Morozova, A.V. Yurkovskaya, Y.P. Tsentalovich, R.Z. Sagdeev, T. Wu, M.D.E. Forbes, *J. Phys. Chem. A* 101 (1997) 8803-8808.
- [9] Y.P. Tsentalovich, O.B. Morozova, N.I. Avdievich, G.S. Ananchenko, A.V. Yurkovskaya, J.D. Ball, M.D.E. Forbes, *J. Phys. Chem. A* 101 (1997) 8809-8816.
- [10] Y.P. Tsentalovich, M.D.E. Forbes, O.B. Morozova, I.A. Plotnikov, V.P. McCaffrey, A.V. Yurkovskaya, *J. Phys. Chem. A* 106 (2002) 7121-7129.
- [11] I. Suzuki, R. Tanaka, A. Yamaguchi, S. Maki, H. Misawa, K. Tokumaru, R. Nakagaki, H. Sakuragi, *Bull. Chem. Soc. Jpn.* 72 (1999) 103-113.
- [12] U. Steiner, T. Ulrich, *Chem. Rev.* 89 (1989) 51-147, and references cited therein.
- [13] R. Nakagaki, K. Mutai, M. Hiramatsu, H. Tukada, S. Nagakura, *Can. J. Chem.* 66 (1988) 1989-1996.
- [14] R. Nakagaki, Y. Tsujimoto, K. Mutai, *Chem. Phys. Lett.* 244 (1995) 388-394.
- [15] R. Nakagaki, K. Mutai, *Bull. Chem. Soc. Jpn.* 69 (1996) 261-274, and references cited therein.
- [16] R. Nakagaki, S. Kohtani, in: M. Yamaguchi, Y. Tanimoto (Eds.), *Magneto-Sciences: Fundamental and Applications on Magnetic Field Effects on Materials*, Kodansha/Springer, Tokyo, 2006, Section 1.4.
- [17] A.A. Baum, *Tetrahedron Lett.* 18 (1972) 1817-1820.
- [18] S. Kohtani, M. Sugiyama, Y. Fujiwara, Y. Tanimoto, R. Nakagaki, *Bull. Chem. Soc. Jpn.* 75 (2002) 1223-1233.

- [19] J.N. Murrell, *The Theory of the Electronic Spectra of Organic Molecules*, Chapman and Hall, 1963, Chap. 8.
- [20] S.L. Murov, I. Carmichael, G.L. Hug, *Handbook of Photochemistry*, second ed. Revised and Expanded, Marcel Dekker, 1993, Section 12.3.
- [21] M. Buback, S. Klingbeil, J. Sandmann, M.B. Sderra, H. P. Vögele, H. Wackerbarth, L. Wittkowski, *Z. Phys. Chem.* 210 (1999) 199-221.
- [22] M. Buback, J. Sandmann, *Z. Phys. Chem.* 214 (2000) 583-607.
- [23] M. A. Miranda, E. Font-Sanchis, J. Perez-Prieto, *J. Org. Chem.*, 64 (1999) 3802-3803.
- [24] J. K. Vollenweider, H. Paul, *Int. J. Chem. Kinet.* 18 (1986) 791-800.
- [25] F.J.J. de Kanter and R. Kaptein, *J. Am. Chem. Soc.*, 104 (1982) 4759-4766.
- [26] R. Nakagaki, M. Yamaoka, K. Mutai, *Bull. Chem. Soc. Jpn.*, 72 (1999) 347-355.

Figure captions

Figure 1 Absorption and CD spectra of 2PCDD in hexane in near UV region (230-340nm). The faster effluent enantiomers of 2PCDD on the Chiral-HPLC is indicated by thin line (fast) in CD spectra. The slower one for 2PCDD is also indicated by solid lines (slow).

Figure 2 Dependence of ISC rate constants (k_{ISC}) on external magnetic fields. The axis of ordinate is the ratio of k_{ISC} in field strengths (k_{MF}) to k_{ISC} at 0 mT (k_{0T}).

Figure 3 Total ion chromatogram for 2PCDD in the air-saturated hexane solution photolyzed with steady-state irradiation for 10 min. The irradiation experiment was performed using the high pressure Hg lamp equipped with a Toshiba UV 29 cut-off filter.

Figure 4 Time profiles of decomposition of 2PCDD (\blacklozenge) and formation of product 1 (\square), product 2 (\triangle), benzaldehyde (\circ), cyclodecane (\bullet), acetophenone (\times), and cyclophane ($*$) in air-saturated hexane solution upon the irradiation with the high pressure Hg lamp equipped with a Toshiba UV 29 cut-off filter.

Figure 5 Time evolution of 2PCDD enantiomer concentration started from optical pure enantiomer (\circ) upon the irradiation with pulsed linearly polarized light (308nm, $0.35\text{mJ cm}^{-2}\text{ pulse}^{-1}$, fwhm ca. 14ns). Curve fitting were made by numerical integration using the Runge-Kutta method with the following parameters: $I_0\eta = 6.3 \times 10^{-8}\text{einstein}\cdot\text{cm}^{-2}\text{s}^{-1}$, $\epsilon = 107\text{ M}^{-1}\text{cm}^{-1}$, $k_{ISC} = 1.3 \times 10^7\text{s}^{-1}$, $k_{ESC}[\text{O}_2] = 1.4 \times 10^7\text{s}^{-1}$, and $\phi = 0.25$, where I_0 is an incident light intensity, ϵ is the molar extinction coefficient of 2PCDD at 308 nm, η is a quantum yield of ^3BR generated from the excited 2PCDD, and ϕ is a recombination yield from ^1BR to each 2PCDD enantiomer.

Table 1 The concentrations of 2-Phenyl-1-oxacyclododecane (Product **1**) and Phenylcycloundecane (product **2**) as well as the relative peak intensities of cyclophane (product **3**) produced in the steady state photolysis in the presence and absence of a magnetic field. The product yields are indicated in the parentheses. The extent of sample decomposition was ca. 80%.

External magnetic field strength / mT	Phenylcycloundecane (2) / 10 ⁻⁶ M (yield)	2-phenyl-1-oxacyclododecane (1) / 10 ⁻⁴ M (yield)	Cyclophane (3)
0	1.60±0.12 (0.0008)	2.75±0.26 (0.14)	1.00±0.22
5	1.61±0.19 (0.0008)	2.72±0.32 (0.14)	1.01±0.12
600	1.56±0.08 (0.0008)	2.69±0.26 (0.14)	0.91±0.09

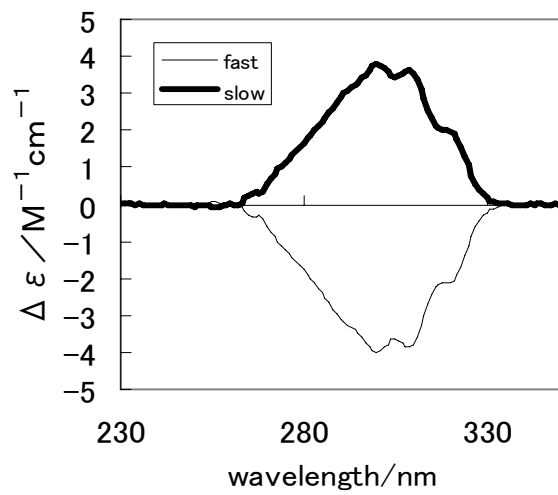
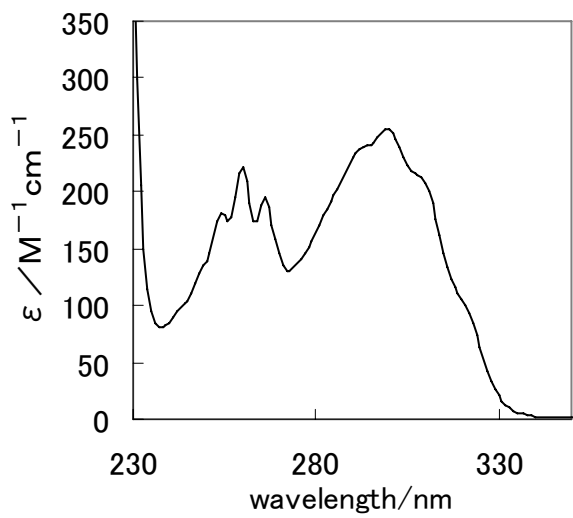


Figure 1 Takahashi et al.

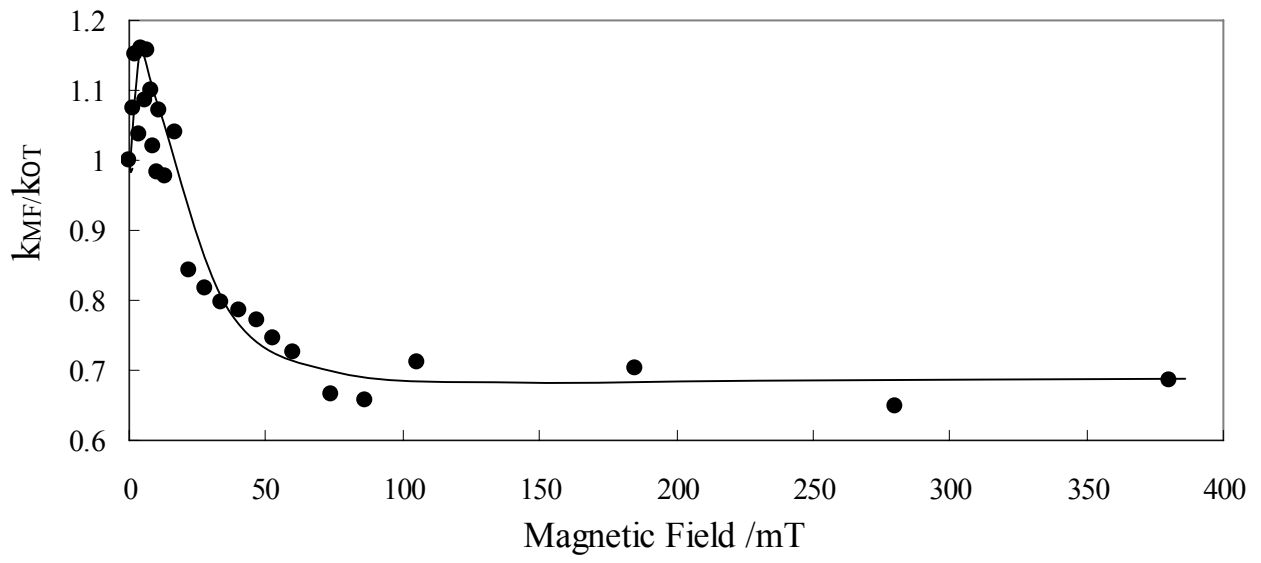


Figure 2 Takahashi et al.

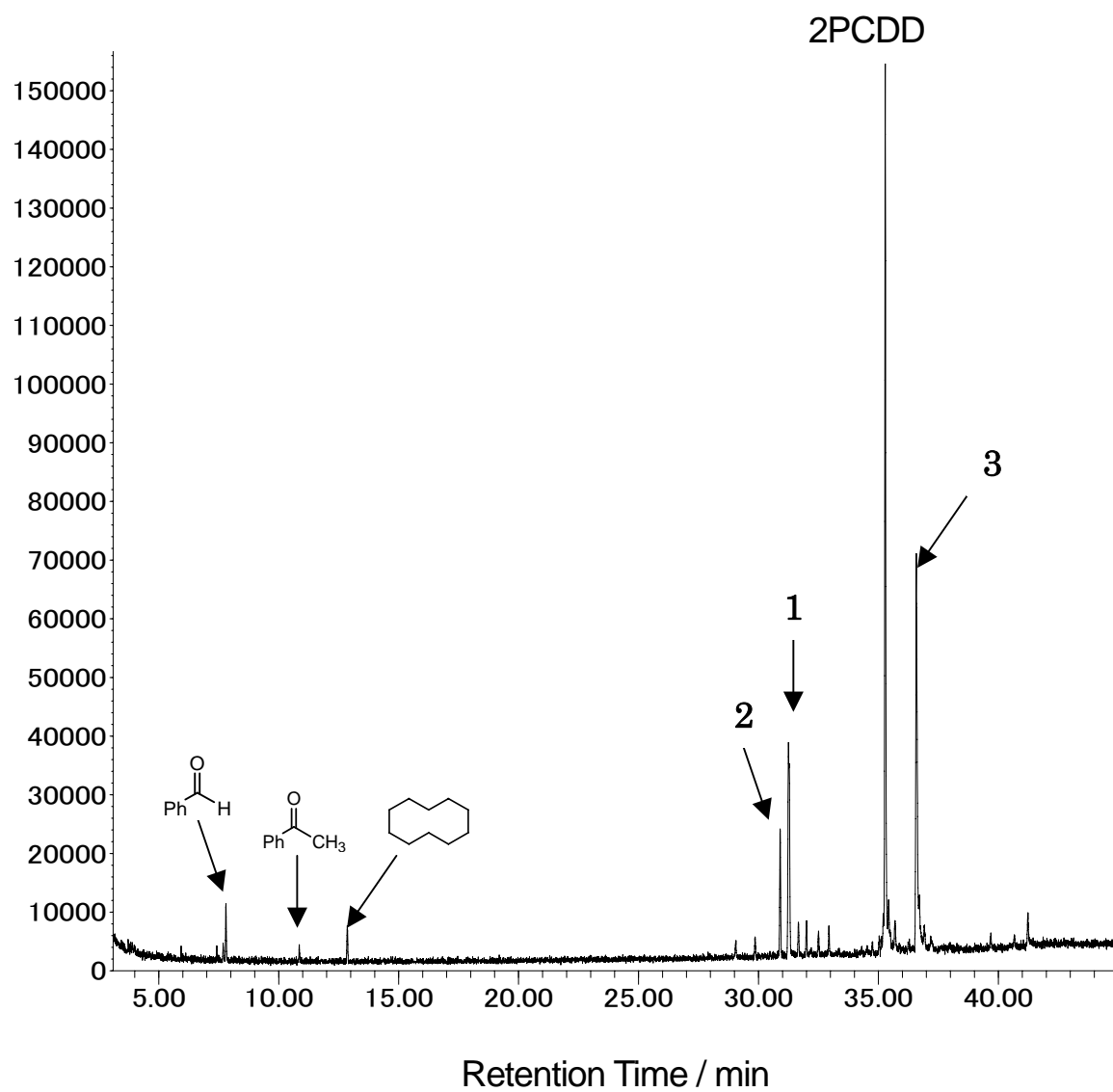


Figure 3 Takahashi et al.

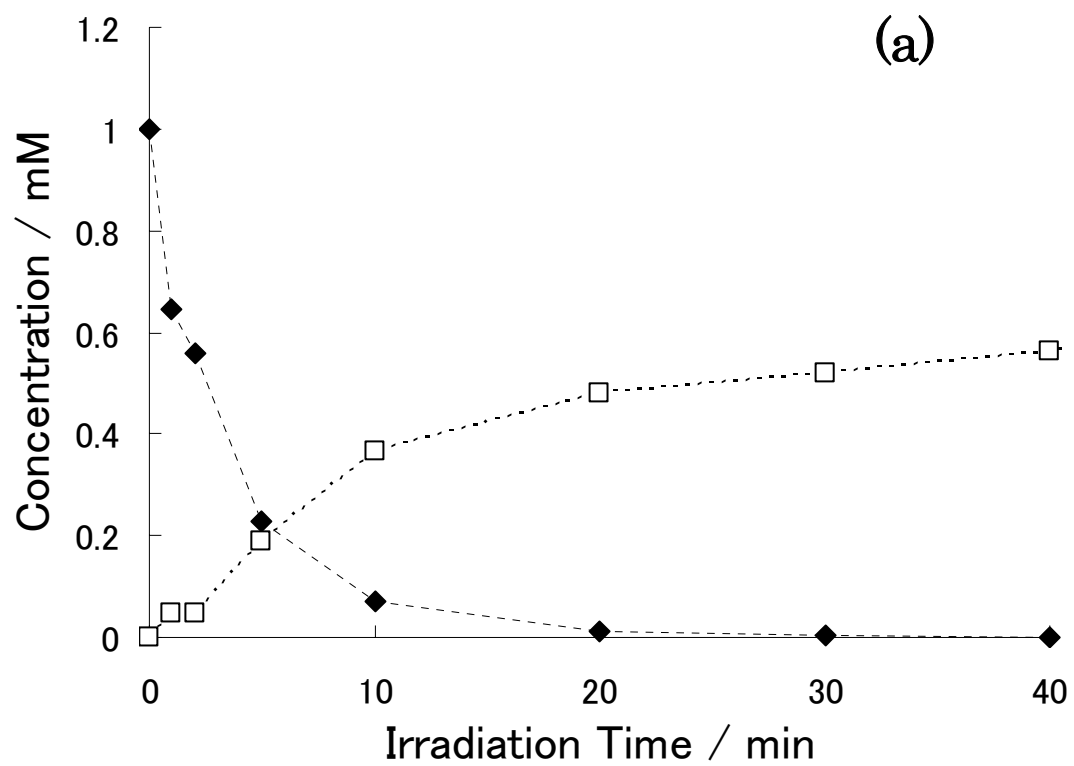


Figure 4 (a) Takahashi et al.

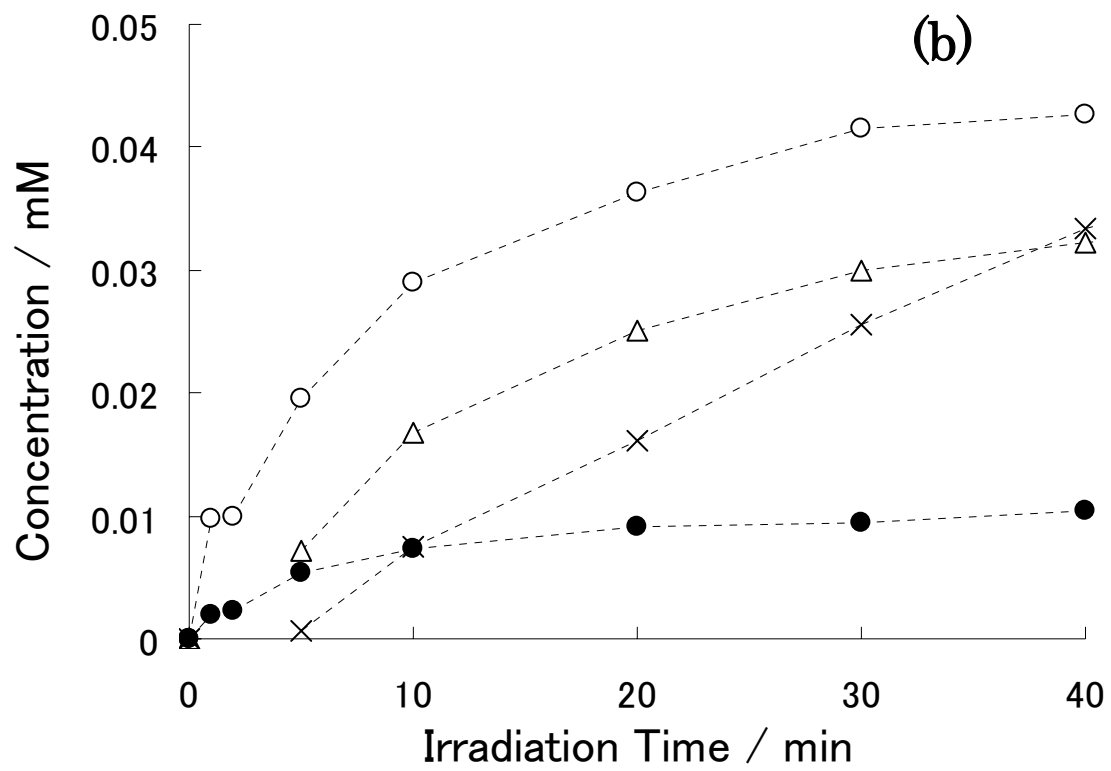


Figure 4 (b) Takahashi et al.

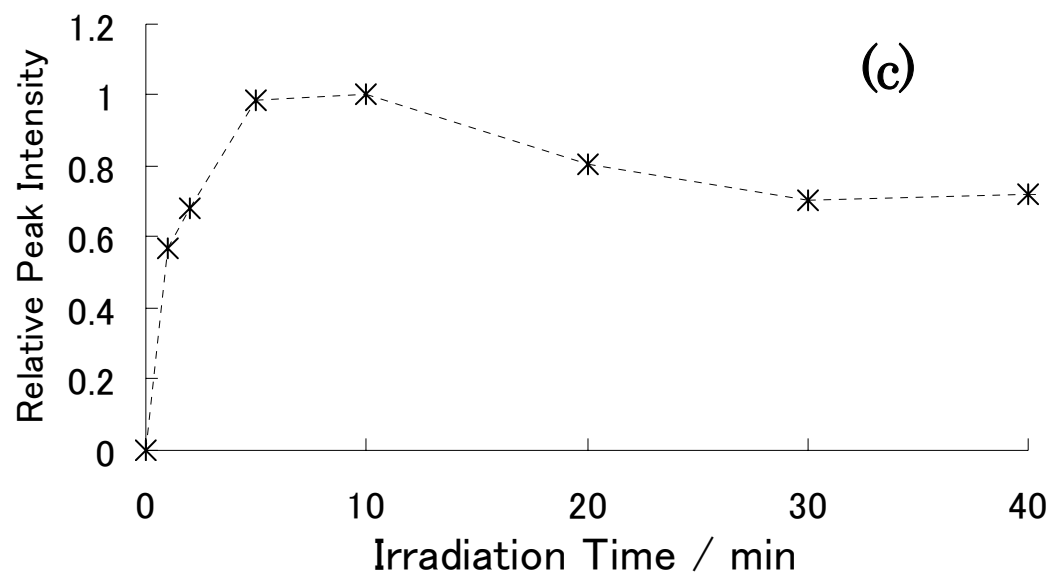


Figure 4 (c) Takahashi et al.

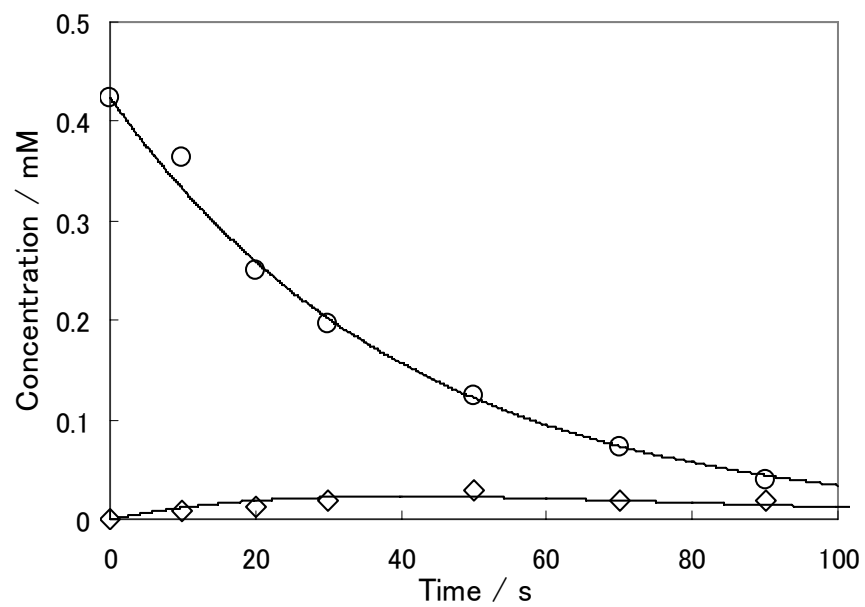
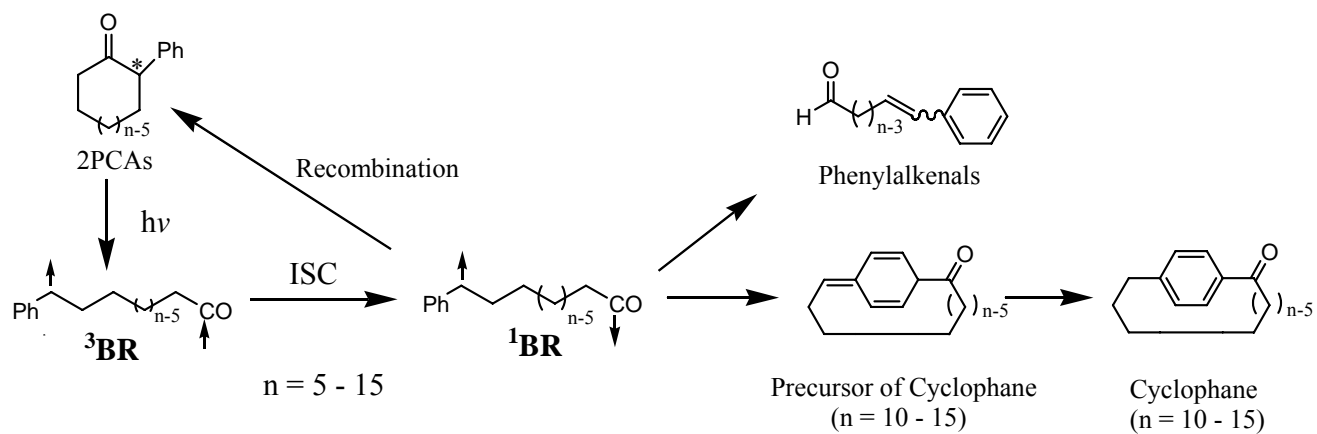
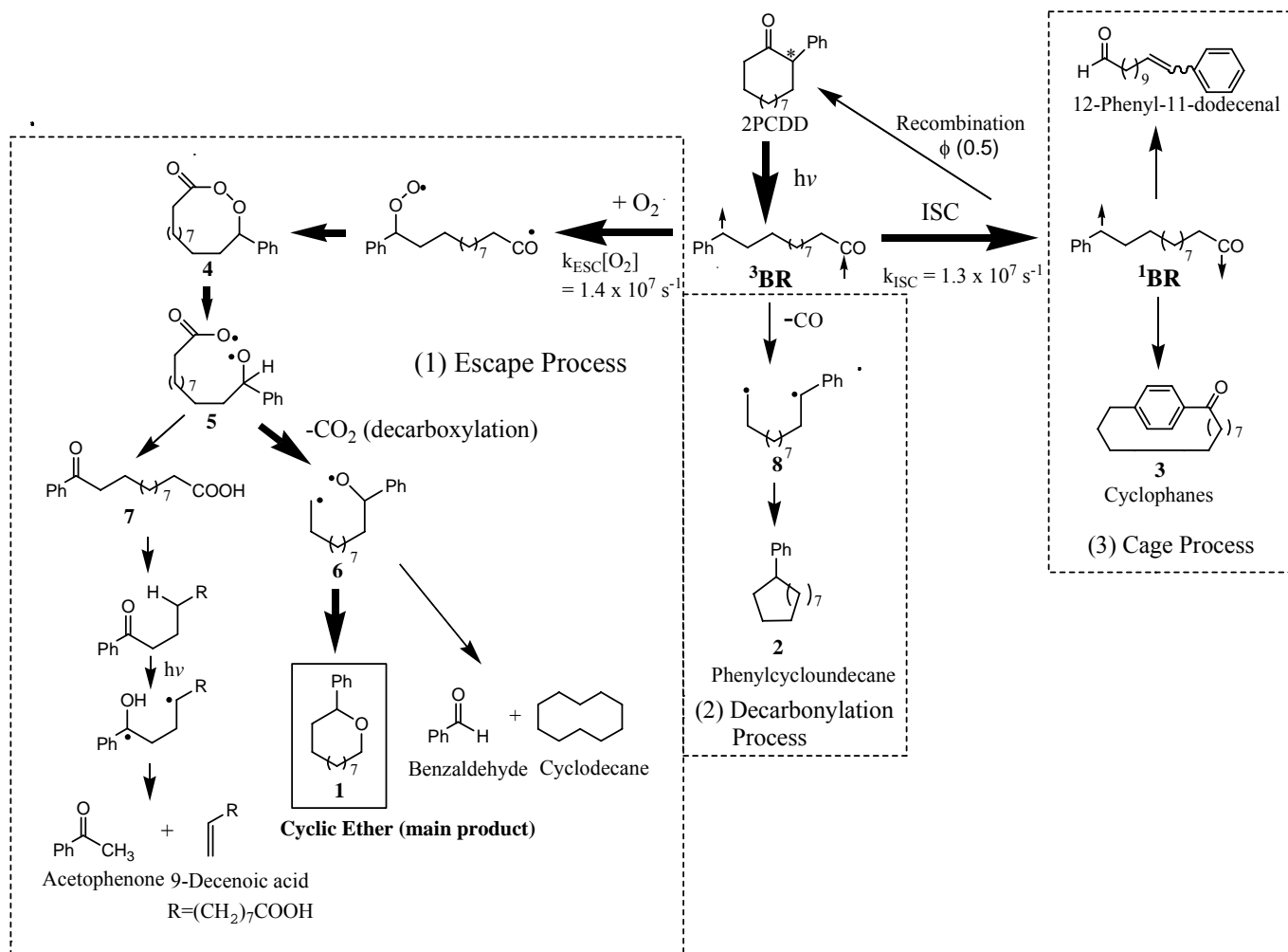


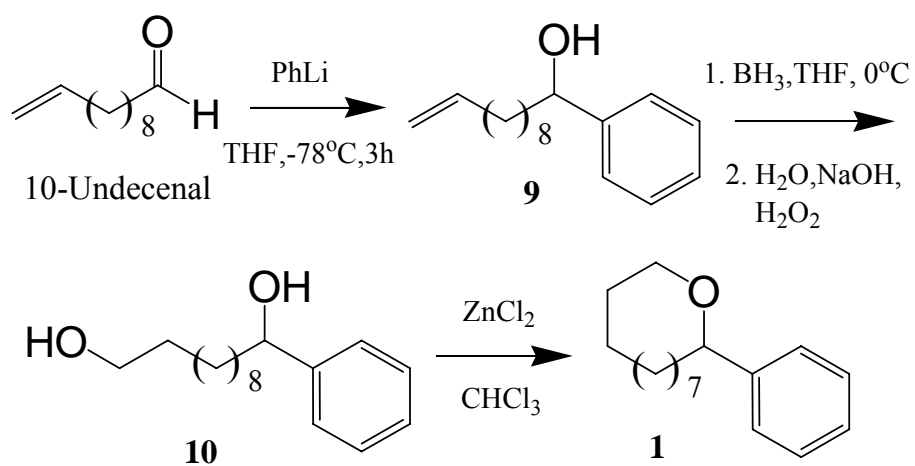
Figure 5 Takahashi et al.



Scheme 1 Takahashi et al.



Scheme 2 Takahashi et al.



Scheme 3 Takahashi et al.